学位論文

Systemically Administered D-allose Inhibits the Tumor Energy Pathway and Exerts Synergistic Effects With Radiation

香川大学大学院医学系研究科

医学専攻

寒川　泰

ANTICANCER RESEARCH *44*: 1895-1903 (2024)
doi:10.21873/anticanres.16991

Systemically Administered D-allose Inhibits the Tumor Energy Pathway and Exerts Synergistic Effects With Radiation

YASUSHI SAMUKAWA[1], YOHEI OUCHI[1], TAKENORI MIYASHITA[1], ASADUR RAHMAN[2], IKUKO TSUKAMOTO[3], AKIHIDE YOSHIHARA[4] and HIROSHI HOSHIKAWA[1]

[1]*Department of Otolaryngology, Faculty of Medicine, Kagawa University, Kagawa, Japan;*
[2]*Department of Pharmacology, Faculty of Medicine, Kagawa University, Kagawa, Japan;*
[3]*Department of Pharmaco-Bio-Informatics, Faculty of Medicine, Kagawa University, Kagawa, Japan;*
[4]*International Institute of Rare Sugar Research and Education & Faculty of Agriculture, Kagawa University, Kagawa, Japan*

Abstract. *Background/Aim: The present study investigated the anticancer effects of intraperitoneally administered D-allose in in vivo models of head and neck cancer cell lines. Materials and Methods: To assess the direct effects of D-allose, its dynamics in blood and tumor tissues were examined. Results: D-allose was detected in blood and tumor tissues 10 min after its intraperitoneal administration and then gradually decreased. In vivo experiments revealed that radiation plus D-allose was more effective than either treatment alone. Thioredoxin-interacting protein (TXNIP) mRNA over-expression was detected after the addition of D-allose in in vitro and in vivo experiments. D-allose inhibited cell growth, which was associated with decreases in glycolysis and intracellular ATP levels and the prolonged activation of AMPK. The phosphorylation of p38-MAPK was also observed early after the administration of D-allose and was followed by the activation of AMPK and up-regulated expression of TXNIP in both in vitro and in vivo experiments. Conclusion: Systemically administered D-allose appears to exert antitumor effects. Further studies are needed to clarify the appropriate dosage and timing of the administration of D-allose and its combination with other metabolic agents.*

D-allose, a rare sugar, has been shown to exert antitumor effects in various types of cancer cells (1-3). Yamaguchi *et al.* (4) reported the gene expression profiles of HuH-7 cells (human hepatocellular carcinoma) treated with D-allose using a microarray technique. There were 37 up-regulated and 11 down-regulated genes. Among the 37 up-regulated genes, thioredoxin-interacting protein (TXNIP), which is a tumor suppressor, showed the most significant increases. Based on these findings, D-allose acts as a novel anticancer agent via the unique induction of TXNIP and p27kip1 protein stabilization. We previously examined the antitumor effects of D-allose in head and neck squamous cell carcinoma (HNSCC) and demonstrated that TXNIP was over-expressed in tumor cells following its administration (5). Thioredoxin acts as a potent antioxidant and redox regulator (6). Its over-expression has been detected in various cancer types (7-9) and is associated with a poor prognosis (9-11). In contrast, TXNIP is down-regulated in various cancer types and correlates with a poor prognosis (12,13). Therefore, D-allose, which up-regulates the expression of TXNIP in cancer cells, has potential as an antitumor agent. However, it currently remains unclear whether the systemic administration of D-allose exerts antitumor effects in *in vivo* models. We previously demonstrated that a local injection of D-allose inhibited tumor growth in an *in vivo* model (5, 14). HNSCC, such as oral and oropharyngeal cancer, and skin cancer are easily visible and palpable. Although the local administration of antitumor agents is not suitable for many cancer types, it represents a good treatment option for HNSCC and skin cancer. The systemic administration of 2-deoxyglucose (2DG), a glycolytic inhibitor, has been reported to suppress the proliferation of cancer cells (15, 16), and trials for its clinical application have been indicated (17, 18). Systemic administration is essential not only for treating cancers in other organs but also for head and neck cancer, as challenging areas exist that cannot be reached solely through local administration. The pharmacokinetics of systemic administration and local injections differ markedly. Although the antitumor effects of a local injection of D-allose have

Correspondence to: Dr. Hiroshi Hoshikawa, Department of Otolaryngology, Faculty of Medicine, Kagawa University, 1750-1 Ikenobe, Miki-cho, Kita-gun, Kagawa 761-0793, Japan. E-mail: hoshikawa.hiroshi.tu@kagawa-u.ac.jp

Key Words: D-allose, head and neck cancer, AMPK, TXNIP, glycolytic system.

been examined, those of its systemic administration *in vivo* remain unknown. Therefore, we herein used an *in vivo* model to investigate whether D-allose was transferred to blood and tumor tissues following its intraperitoneal administration and exerted antitumor effects when administered via this route. We also assessed the effects of D-allose on glycolytic stress, changes in ATP production, and signaling pathways.

Materials and Methods

Cell culture. The human head and neck carcinoma cell line HSC3 (tongue carcinoma) was obtained from the Health Science Research Resources Bank, Osaka, Japan. The cell line was grown in Eagle's minimal essential medium (EMEM) with 10% heat-inactivated fetal bovine calf serum and 1% penicillin-streptomycin. Cells were incubated at 37°C in a humidified atmosphere with 5% CO_2.

Analysis of biodistribution. Twelve mice were divided into four groups (3 each). Blood samples and tumor tissues were collected after 10, 30, 60, and 90 min of administration. To investigate the blood concentrations of D-allose and D-glucose, D-allose was assayed using high-performance anion-exchange chromatography with pulsed amperometric detection (HPAE-PAD). Dionex ICS300 and the CarboPack PA1 column (DionexTM, Tokyo, Japan) were used. Blood samples were deproteinized by mixing with four-fold volumes of EtOH. After centrifugation, supernatants were filtered (0.45 μm) and then applied to HPAE-PAD. A 25-μl sample was added to the column set at 35°C and eluted with 1 ml/min of 10 mM NaOH. The quantitative relationship between sugar concentrations and peak areas (nC•min) was confirmed within the range of 1 to 500 mg/l. To investigate the tissue concentrations of D-allose and D-glucose, a 10-μl sample was added to 40 μl of 4-aminobenzoic acid ethyl ester (ABEE) reagent (J-CHEMICAL Inc., Tokyo, Japan), and the mixture was heated at 80°C for 1 h. After cooling to room temperature, 200 μl of distilled water and 200 μl of chloroform were added to the mixture. The mixture was centrifuged at 800 × *g* for 5 min and the upper layer was used for a high-performance liquid chromatography (HPLC) analysis.

ABEE-labeled samples were analyzed by HPLC using the XBridge C18 column (Waters Corp. Milford, MA, USA) at 30°C, which was eluted with 0.2 M potassium borate buffer (pH 8.9) and acetonitrile (93:7) at a flow rate of 1.0 ml/min. Eluted samples were detected using a fluorescence monitor (excitation wavelength of 305 nm and emission wavelength of 360 nm).

Xenograft model experiment. D-allose was supplied by the Department of Biochemistry and Food Science, the Faculty of Agriculture, Kagawa University, Kagawa, Japan. D-allose was dissolved in saline to an appropriate concentration. HSC3 cells were used in a xenograft model with female athymic nude mice (BALB/c nu/nu, 5-6 weeks old). Each mouse was subcutaneously injected with 1×10^6 cells in 0.1 ml EMEM on the right side of the posterior flank using a 1-cc syringe with a 27G needle. Tumors were grown for ten days until an average size of 100 mm^3 was attained (day 0). To assess the antitumor effects of the intraperitoneal injection of D-allose and investigate the combined effects of radiation, 24 mice were randomly divided into four groups. The four groups were treated as follows: with the intraperitoneal administration of 0.2 ml of normal saline 5 times a week (control), with the intraperitoneal administration of 0.2 ml of 50 mM D-allose 5 times a week (allose), with a 4-Gy dose of irradiation 2 times a week (RT), or with the intraperitoneal administration of 0.2 ml of 50 mM D-allose 5 times a week plus a 4-Gy dose irradiation 2 times a week (RT + allose). The duration of treatment was 3 weeks in each group (until day 21). Tumor sizes were monitored for 5 weeks (until day 35). The posterior flank sites of mice into which tumors were implanted were irradiated using an X-ray irradiator (HITEX type HW 260, 200 kV, 5 mA, Osaka, Japan). All mice were euthanized with an intraperitoneal injection of 240 mg/kg body weight of ketamine hydrochloride and 30 mg/kg body weight of xylazine. The duration of the experiment was from January 30 to March 24, 2023. The present study was approved by the Animal Care and Use Committee of Kagawa University (Approval No. 21658-1, Approval Date January 20, 2023).

Analysis of mRNA expression. To investigate the effects of D-allose on the mRNA expression of TXNIP *in vitro*, cells were cultured in 6-cm dishes with 50 mM D-allose for 24 h. To examine the effects of D-allose on the expression of TXNIP *in vivo*, the xenograft mice described above were intraperitoneally administered 0.2 ml of 100 mM D-allose, and tumors were removed 48 h later. Total RNA was isolated using a NucleoSpin RNA kit (Macherey-Nagel, Duren, Germany), and cDNA was synthesized using a SuperScript III kit (Invitrogen, Waltham, MA, USA). A real-time polymerase chain reaction (PCR) was performed using TaqMan gene expression assay primers (Hs00197750_m1, GAPDH: Hs99999905_m1) and the ABI ViiA7 RealTime PCR system (Applied Biosystems, Waltham, MA, USA). The *GAPDH* gene was used to normalize expression across assays and runs, and a quantification value (Cq) for each sample was used to assess the expression level of the gene.

Western blot analysis. Cells were cultured in 10-cm dishes under 70% confluency, and after treatment with 50 mM D-allose for 20 min, 40 min, 6 h, and 24 h, they were scraped into SDS sample buffer containing dithiothreitol (EzApply, ATTO Corp., Tokyo, Japan). Samples were then heated at 95°C for 5 min.

In *in vivo* experiments, proteins were extracted from the tumor tissues of xenograft mice after the intraperitoneal administration of 0.2 ml of 100 mM D-allose. Tumor tissues were washed with PBS, placed in lysis buffer (50 mM Tris-HCl, pH 7.5, 150 mM NaCl, 0.5% Triton-X100, and 0.5% NP-40) containing protease inhibitor cocktail (Sigma-Aldrich, St. Louis, MO, USA), and sonicated. Samples were centrifuged at 20,000 × *g* at 4°C for 10 min, and the supernatants were collected.

In western blot analyses, proteins were separated on 10% SDS-PAGE gels, transferred to nitrocellulose membranes, blocked with 5% (w/v) nonfat dried milk in PBS, and incubated with antibodies against TXNIP mouse mAb (K0205-3, MBL, Nagoya, Japan), β-Actin mouse mAb (M177-3, MBL), P38 MAPK rabbit mAb (#9212, Cell Signaling Technology, Inc., Tokyo, Japan), phospho-P38 MAPK rabbit mAb (#9211, Cell Signaling), AMPKα rabbit mAb (#2532, Cell Signaling), or phospho-AMPKα rabbit mAb (#2531, Cell Signaling). Membranes were probed with horseradish peroxidase-conjugated anti-mouse IgG (NA931, Amersham, Tokyo, Japan) or anti-rabbit IgG (#7074, Cell Signaling), and signals were detected using an enhanced chemiluminescence system (Amersham).

Glycolytic stress test and real-time ATP rate assay. The cellular glycolytic capacity and real-time ATP production rate were evaluated using the Agilent Seahorse XF HS Mini Extracellular Flux Analyzer (Seahorse Bioscience; Agilent Technologies, North

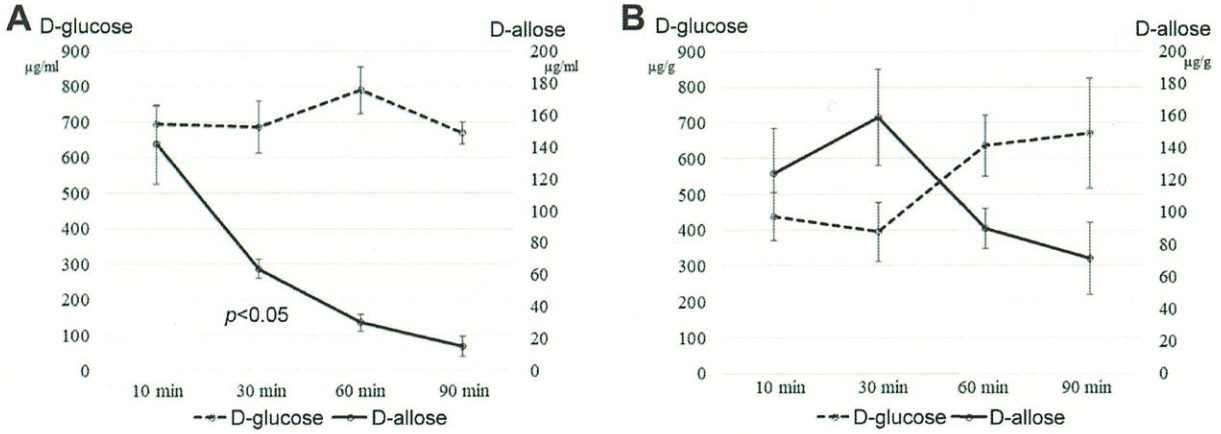

Figure 1. *Distribution of D-allose into blood and tumor tissues after its intraperitoneal administration. Error bars represent standard errors. (A) Blood concentrations of D-glucose and D-allose were measured over time after the administration of D-allose. The Kruskal–Wallis test revealed significant changes in blood concentrations of D-allose ($p<0.05$). (B) D-glucose and D-allose concentrations in tumor tissues were measured after the administration of D-allose. D-allose was detected in tumors after 10 min and peaked at 30 min.*

Billerica, MA, USA), according to the manufacturer's instructions included in the Agilent Seahorse XFp Glycolysis Stress Test kit and XFp Real-Time ATP rate assay kit, respectively. HSC3 cells were cultured in Dulbecco's modified Eagle's medium (DMEM) supplemented with FBS (10%). Cells were plated into an XF HS Mini cell culture plate at a density of 2.0×10^4 cells per well, maintained for 24 h, and serum-starved at 37°C for the next 18 h in a CO_2 incubator. Prior to starting the assay, compounds (2 mM glutamine for the glycolysis stress test; 10 mM glucose, 1 mM pyruvate, and 2 mM glutamine for the ATP rate assay) were diluted to the appropriate concentrations in freshly prepared assay medium (Seahorse XF DMEM Medium, pH 7.4). The medium in the plate with cells was then changed to assay medium and maintained in a non-CO_2 incubator at 37°C for 1 h prior to the assay. In both assays, following the measurement of basal values, vehicle (assay medium) or D-allose (50 mM) was injected from the first port and incubated for 30 min. The glycolysis stress test was then conducted by injecting glucose (10 mM), oligomycin (1 μM), and 2-DG (50 mM) at 18-min intervals; and the ATP rate assay by injecting oligomycin (1.5 μM) and rotenone/antimycin A (0.5 μM) at 30-min intervals. At the end of the assay, the solution in the wells was removed, and 30 μl of lysis buffer was added and vortexed to lyse cells. Total protein levels in each well were measured using the Bradford assay. Results were analyzed with Seahorse Wave software (Seahorse Bioscience) and normalized with protein concentrations.

Statistical analysis. Statistical analyses were performed using StatFlex V6.0 (Artec Co. Ltd., Osaka, Japan). The Kruskal–Wallis test was used to compare changes in blood and tissue concentrations over time. Comparisons of tumor volumes between the treatment and control groups were conducted using the Newman–Keuls test. mRNA expression levels were compared between the control and D-allose treatment groups using the Student's *t*-test. Changes in the glycolytic system were compared using the Student's *t*-test. A *p*-value of <0.05 was considered to indicate a significant difference.

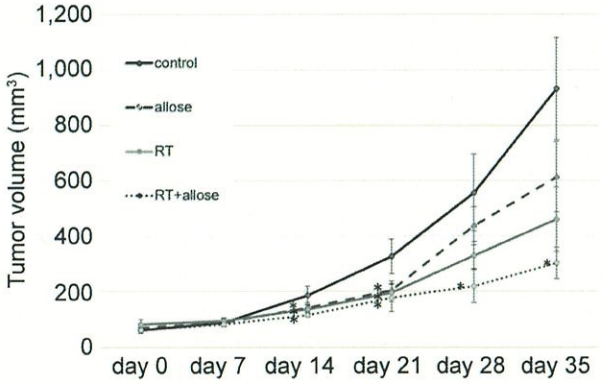

Figure 2. *Changes in tumor sizes in xenograft mice in various treatment groups. Tumor volumes (mm^3) after the intraperitoneal administration of 0.2 ml of 50 mM D-allose 5 times a week for three weeks. Points: mean tumor volume; error bars: standard errors. Significant differences are indicated by asterisks: *$p<0.05$ vs. the control group.*

Results

Absorption of D-allose into blood and tumor tissues. Intraperitoneally administered D-allose was quickly transferred into the blood within 10 min. Thereafter, it gradually decreased and almost disappeared after 90 min. The Kruskal–Wallis test showed a significant change in the blood concentration of D-allose ($p<0.05$). The blood concentration of D-glucose was maintained at approximately 700 μg/ml in the presence of D-allose. D-allose was also detected in tumor tissues after 10 min, peaked at 30 min, and then gradually decreased. D-Glucose

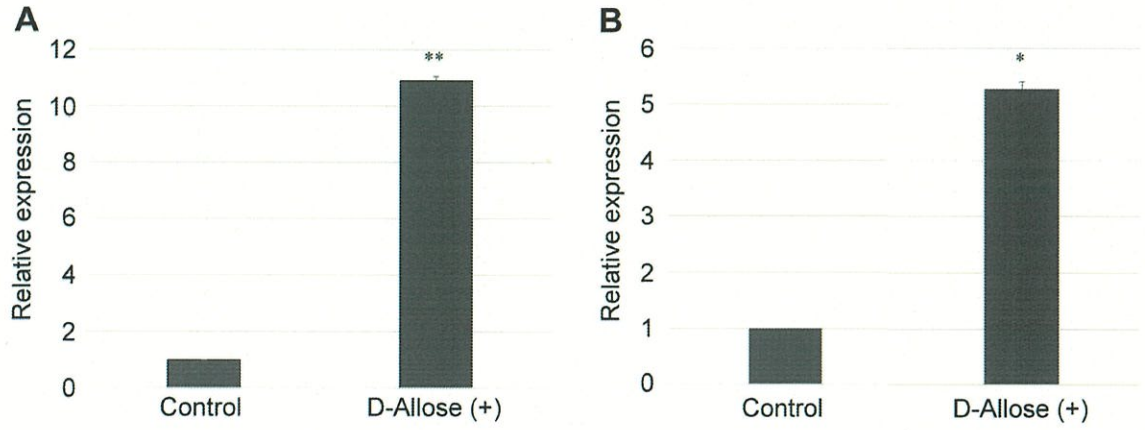

Figure 3. *Changes in TXNIP mRNA expression levels after the treatment with D-allose. Error bars represent standard errors. (A) Experiments on cultured cells showed an approximately 10-fold increase in expression levels from the control group 24 h after treatment. **p<0.01 vs. the control group. (B) An approximately 5-fold increase in expression levels from those in the control group was observed 48 h after the intraperitoneal administration of D-allose. *p<0.05 vs. the control group.*

concentrations in tumor tissues slightly decreased in the presence of D-allose (Figure 1).

Effects of the intraperitoneal administration of D-allose and irradiation. Tumor volumes were significantly smaller in the group intraperitoneally administered D-allose than in the control group from days 14 to 21 after administration ($p<0.05$). Tumor volumes were significantly smaller in the irradiated group than in the control group on day 21 ($p<0.05$), and suppressive effects on growth were enhanced by the combined use of D-allose on days 21 to 35 ($p<0.05$) (Figure 2).

Changes in TXNIP mRNA expression levels by the intraperitoneal administration of D-allose. In the *in vitro* experiment, TXNIP mRNA expression levels significantly increased ($p<0.01$, 11-fold increase 24 h after the addition of D-allose). In the *in vivo* experiment, TXNIP mRNA expression levels in tumor tissues 48 h after the intraperitoneal administration of D-allose also significantly increased by more than 5-fold ($p<0.05$) (Figure 3).

Effects of D-allose on MAPK and AMPK kinase systems. To elucidate the effects of D-allose treatment on intracellular signaling pathways, we examined changes in the levels and activation of proteins involved in the MAPK and AMPK kinase pathways. In cultured cells, the phosphorylation of p38-MAPK was observed early after the administration of D-allose and was followed by the phosphorylation of AMPK and the up-regulated expression of TXNIP (Figure 4).

The phosphorylation of p38-MAPK was also detected early in tumor tissues, while the phosphorylation of AMPK and expression of TXNIP were observed after 48 h (Figure 5).

Effects of D-allose on the glycolytic system. Glucose metabolism was examined by measuring the extracellular acidification rate (ECAR). In comparisons with the control group, glucose metabolism ($p<0.05$) and the glycolytic capacity ($p<0.01$) were significantly suppressed 30 min after the administration of 50 mM D-allose, reflecting a change in the glycolytic system (Figure 6). No significant differences were observed in glycoATP (production of glycolysis-derived ATP) or mitoATP (mitochondrial production of ATP) between the groups (Figure 7).

Discussion

In the present study, we initially demonstrated the distribution of D-allose in blood and tumor tissues following its intraperitoneal administration. Intraperitoneally administered D-allose was rapidly transferred into blood and then gradually decreased. In contrast, D-allose administered intraperitoneally was rapidly transferred into tumor tissues and was maintained at high concentrations. D-allose and D-glucose have been suggested to compete in tumor tissues based on previous findings showing that D-allose suppressed the cellular uptake of D-glucose (19). A similar response may occur at the tissue level.

Although D-allose inhibited the proliferation of several types of cancer cells (1-3), it currently remains unclear whether it has similar effects *in vivo* following its oral and intravenous administration. The present study confirmed that D-allose was transferred into blood and tumor tissues following its intraperitoneal administration. Moreover, the intraperitoneal administration of D-allose exerted antitumor effects similar to those of a local injection (5). A previous

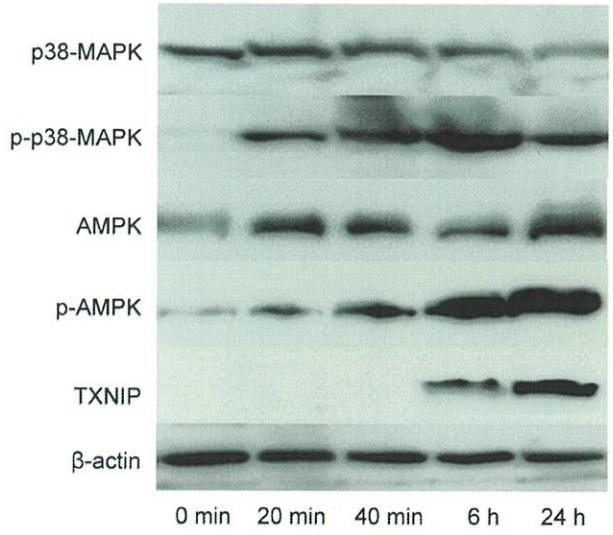

Figure 4. *Expression of p38-MAPK, p-p38-MAPK, AMPK, p-AMPK, and TXNIP at 0 min, 20 min, 40 min, 6 h, and 24 h after the treatment with 50 mM D-allose, as analyzed using western blotting of protein extracts from cultured cells.*

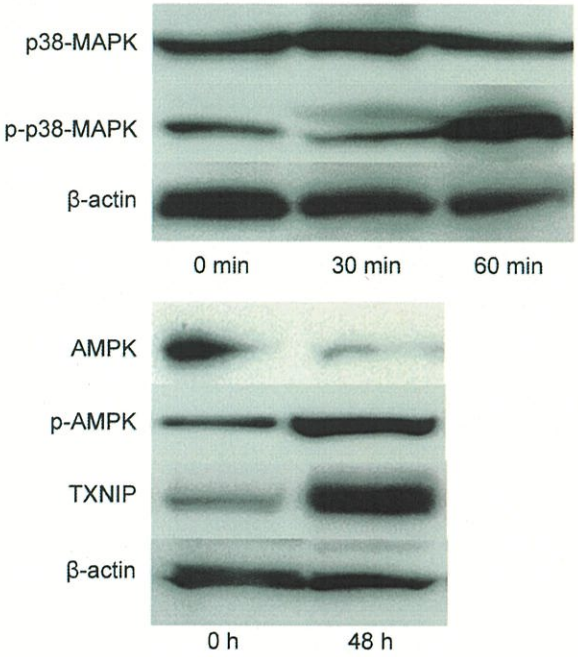

Figure 5. *Western blot analysis in vivo. Proteins were obtained from the tumors of xenograft mice treated with the intraperitoneal administration of 0.2 ml of 100 mM D-allose. The expression levels of p38-MAPK and p-p38-MAPK at 0, 30, and 60 min and AMPK, p-AMPK, and TXNIP levels at 0 and 48 h were analyzed.*

study demonstrated that local injections of 500 mM D-allose into tumors for 3 weeks continued to inhibit tumor growth after the injections were discontinued (20). In the present study, intraperitoneal administration of 50 mM D-allose for three weeks did not inhibit tumor growth after its discontinuation. Therefore, if anti-tumor effects are to be expected by using D-allose alone, it may be necessary to administer a higher dose or extend the duration of administration. Synergistic effects with the intraperitoneal administration of D-allose and irradiation were also confirmed in *in vivo* experiments in the present study. The over-expression of TXNIP at the mRNA and protein levels was observed in tumor tissues after the intraperitoneal administration of D-allose. The microarray analysis revealed that D-allose significantly up-regulated TXNIP gene expression in hepatocellular cancer cells (4). The over-expression of TXNIP by the D-allose treatment was also reported in several cancer types (1-3, 5, 20, 21). Our previous study (5) revealed that the cell growth inhibition rate correlated with the TXNIP expression rate. A recently developed RNA sequencing analysis has the potential to yield unknown mRNA isoforms and more RNA information than a microarray analysis. Further investigations are needed to clarify the involvement of novel genes other than TXNIP. Noguchi *et al.* (22) showed that the over-expression of TXNIP markedly reduced GLUT1 expression and the suppression of GLUT1 expression inhibited cell growth in three human cancer cell lines: hepatocellular carcinoma (HuH-7), Caucasian breast adenocarcinoma (MDA-MB-231), and neuroblastoma (SH-SY5Y). D-allose-induced increases in TXNIP and TXNIP over-expression-induced decreases in GLUT1 were confirmed in all three cancer cell lines. Furthermore, the knockdown of TXNIP using siRNA canceled the D-allose-induced suppression of GLUT1 expression in HuH-7 cell lines. The knockout of TXNIP also promoted the proliferation of breast cancer cells, which was accompanied by the expression of p27 and increased GLUT1 levels.

2DG has been shown to inhibit tumor growth as a glucose inhibitor. It accumulates in cancer cells and may be phosphorylated by hexokinase to 2-deoxyglucose-6-phosphate (2-DG-6-P). 2-DG-6-P provides negative feedback on hexokinase and inhibits glucose uptake. The inhibition of glycolysis by 2-DG results in glycoATP depletion, which activates AMPK. Previous studies reported that the activation of AMPK signaling suppressed cancer cell proliferation (23-25).

AMPK has been shown to inhibit the activity of mTORC1 in the PI3K/Akt/mTORC1 signaling system and suppress the synthesis of proteins and fatty acids, thereby inhibiting the growth of cancer cells (26).

In an *in vitro* study, the phosphorylation of MAPK and AMPK occurred markedly earlier, approximately 20 min after the administration of D-allose, while TXNIP expression was observed after 6 hours and further increased after 24 h. We hypothesized that phosphorylation and protein expression may

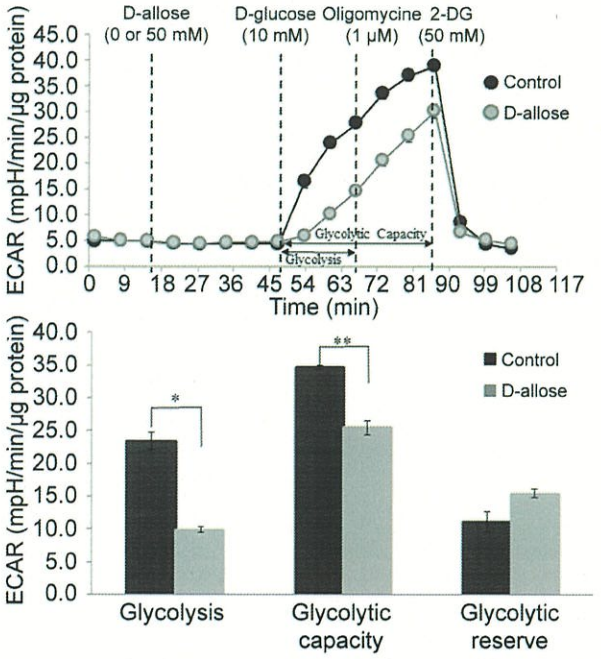

Figure 6. *Changes in ECAR in cultured cells after the administration of D-allose. Error bars represent standard errors. Thirty minutes after the administration of 50 mM D-allose, increases in ECAR were significantly smaller than those in the control group, reflecting changes in glycolysis (*p<0.05) and the glycolytic capacity (**p<0.01).*

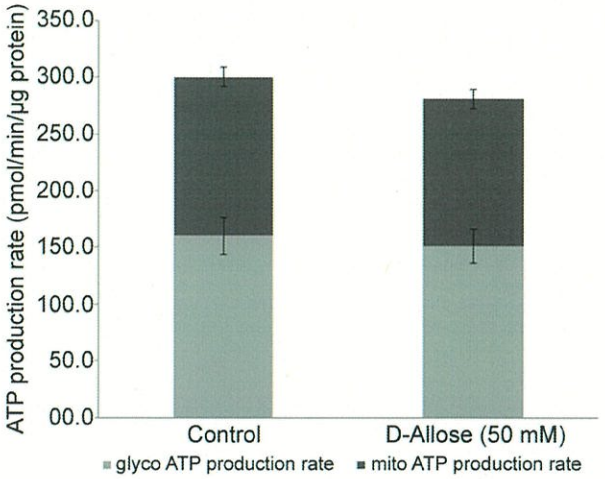

Figure 7. *ATP production rate after the treatment with D-allose. Error bars represent standard errors. No significant differences were observed in the glycoATP or mitoATP production rate from the control group, as analyzed using real-time ATP rate assays.*

take longer than in *in vitro* studies; therefore, tissue was harvested after 48 h in the *in vivo* study to examine protein expression. After 48 h, the phosphorylation of AMPK and TXNIP expression were promoted, suggesting that AMPK was phosphorylated both *in vitro* and *in vivo* after the administration of D-allose, and cell proliferation was subsequently suppressed, which indicated the involvement of AMPK activation in the suppression of cancer cell proliferation. This is the first study to show that D-allose activated AMPK signaling and inhibited tumor growth, similar to 2DG.

A flux analysis revealed that glucose metabolism and glycolytic activity were significantly suppressed in the HSC3 cell line 30 min after the administration of D-allose, while no significant differences were observed in glycoATP or mitoATP between the groups.

In the experiment using the pancreatic cancer cell line, glycoATP markedly decreased, while mitoATP slightly increased 16 h after the administration of D-allose (data not shown). This result suggests that changes in ATP production after the administration of D-allose were affected by time and medium composition. The glycolytic metabolism of cancer is considered to shift to glycolysis. When glycolysis is suppressed, it may shift to energy production by mitochondrial respiration. The oxygen consumption rate (OCR) indicates oxygen consumption due to aerobic respiration, while ECAR measures acidification due to glycolytic metabolism. The measurement of time-dependent changes in OCR and ECAR may help to elucidate the shift in energy production when glycolysis is suppressed.

In the present study, the effects of D-allose on the MAPK pathway were also newly reported. The phosphorylation of p38-MAPK occurred early after the administration of D-allose and was followed by the phosphorylation of AMPK and the up-regulated expression of TXNIP. The stress-responsive MAPK pathway, p38-MAPK, is activated by environmental stress and inflammatory cytokines, and plays a central role in the induction of apoptosis and the regulation of immune responses.

In hepatocellular carcinoma cells, the over-expression of TXNIP inhibited cell proliferation and induced apoptosis by triggering mitochondrial-mediated ROS generation and activating the MAPK pathway (27).

It currently remains unclear whether the phosphorylation of p38-MAPK directly activates AMPK or up-regulates the expression of TXNIP; nevertheless, the activation of the MAPK pathway may have an impact on the antitumor effects of D-allose. However, a previous study reported that the addition of a MAPK inhibitor enhanced the anti-cell proliferation effects of 2DG or D-allose and anticancer drugs (28). Further studies are needed to clarify the possibility of different responses to the activation of MAPK in various cells. We intend to investigate whether MAPK inhibitors suppress the activation of the AMPK pathway and the over-expression of TXNIP in head and neck cancer cell lines in the future.

The findings of studies that combined 2DG with other metabolic regulators, chemotherapeutic agents, and radiation

therapy suggest the potential of 2DG to improve treatment outcomes (29, 30). Metformin is a compound that is widely used to treat type 2 diabetes because it attenuates hyperglycemia by inhibiting hepatic lipogenesis and gluconeogenesis and promotes insulin sensitivity (31). At the cellular level, metformin is a mild mitochondrial complex I inhibitor that decreases ATP levels and AMPK activation. Cheong *et al.* previously reported (32) that 2DG alone was not sufficient to promote cell death. However, 2DG and metformin led to significant cell death associated with decreases in cellular ATP, the prolonged activation of AMPK, and sustained autophagy. Recently, phase III randomized clinical trials have been conducted in several cancer types to clarify the antitumor effects of metformin. As a result, metformin did not reduce the risk of new cancer development in non-diabetic breast cancer patients (33). And there was no significant impact of metformin use on pembrolizumab efficacy in resected high-risk stage III melanoma (34).

We also showed that D-allose enhanced the anti-cell proliferation effects of anticancer drugs and irradiation (14, 20). Therefore, further studies are required to clarify the combined effects of D-allose and other metabolic agents, such as metformin. Although D-allose and 2DG have similar functions, including competition with glucose uptake and the inhibition of glycolysis, D-allose has also been reported to have a different mechanism of action to 2DG, such as stronger effects on TXNIP expression and the inhibition of GLUT1 expression (22). Clinical trials have been performed on 2DG (33-35). However, its effectiveness and safety have not yet been proven.

D-allose is a naturally occurring monosaccharide that is considered to have fewer adverse effects than 2DG. Although the antitumor effects of D-allose as a single agent are limited, its effects in combination with other drugs and irradiation are sufficient for clinical applications. Further studies are needed for the development of more effective administration methods, the selection of optimal doses, and combinations with appropriate drugs and therapies, such as the use of D-allose as an infusion base drug to replace D-glucose when administering anticancer drugs or pre-medication as a radio-sensitizer.

This study has a potential limitation. The present study does not directly confirm whether siRNA-mediated knockdown of TXNIP in head and neck cancer cells cancels effects, such as inhibition of cell proliferation, increase in ROS, and cell cycle arrest. Further studies are needed to clarify the knockdown effect of TXNIP on head and neck cancer cells.

In conclusion, the present results suggest the anticancer effects of the systemic administration of D-allose and a novel mechanism for the activation of the MAPK and AMPK kinase systems and inhibition of glycolysis.

Conflicts of Interest

The Authors declare that they have no competing interests in relation to this study.

Authors' Contributions

YS and YO contributed to experiments, data collection, and analyses of cultured cells and xenograft mice. YS was a major contributor to the writing of the manuscript. TM was involved in statistical analyses of data and critical revisions to the manuscript. AR contributed to analyses of the glycolytic system and ATP. IT analyzed data on the translocation of D-allose into blood. AY analyzed data on the translocation of D-allose into tissues. HH contributed to analyses of mRNA expression and western blotting and gave final approval of the version to be published. All authors read and approved the final manuscript.

Acknowledgements

The Authors appreciate Miss Aiko Ito, a staff member at the Life Science Research Center, Kagawa University for her help.

References

1 Sui L, Dong Y, Watanabe Y, Yamaguchi F, Hatano N, Tsukamoto I, Izumori K, Tokuda M: The inhibitory effect and possible mechanisms of D-allose on cancer cell proliferation. Int J Oncol 27(4): 907-912, 2005.

2 Jeong RU, Lim S, Kim MO, Moon MH: Effect of d-allose on prostate cancer cell lines: phospholipid profiling by nanoflow liquid chromatography–tandem mass spectrometry. Anal Bioanal Chem 401(2): 689-698, 2011. DOI: 10.1007/s00216-011-5113-1

3 Kanaji N, Kamitori K, Hossain A, Noguchi C, Katagi A, Kadowaki N, Tokuda M: Additive antitumour effect of D-allose in combination with cisplatin in non-small cell lung cancer cells. Oncol Rep 39(3): 1292-1298, 2018. DOI: 10.3892/or.2018.6192

4 Yamaguchi F, Takata M, Kamitori K, Nonaka M, Dong Y, Sui L, Tokuda M: Rare sugar D-allose induces specific up-regulation of TXNIP and subsequent G1 cell cycle arrest in hepatocellular carcinoma cells by stabilization of p27kip1. Int J Oncol 32(2): 377-85, 2008.

5 Hoshikawa H, Mori T, Mori N: In vitro and *in vivo* effects of D-Allose: up-regulation of thioredoxin-interacting protein in head and neck cancer cells. Ann Otol Rhinol Laryngol 119(8): 567-571, 2010. DOI: 10.1177/000348941011900810

6 Lu J, Holmgren A: The thioredoxin superfamily in oxidative protein folding. Antioxid Redox Signal 21(3): 457-470, 2014. DOI: 10.1089/ars.2014.5849

7 Cha MK, Suh KH, Kim IH: Overexpression of peroxiredoxin I and thioredoxin1 in human breast carcinoma. J Exp Clin Cancer Res 28(1): 93, 2009. DOI: 10.1186/1756-9966-28-93

8 Lincoln DT, Al-Yatama F, Mohammed FM, Al-Banaw AG, Al-Bader M, Burge M, Sinowatz F, Singal PK: Thioredoxin and thioredoxin reductase expression in thyroid cancer depends on tumour aggressiveness. Anticancer Res 30(3): 767-775, 2010.

9 Zhu X, Huang C, Peng B: Overexpression of thioredoxin system proteins predicts poor prognosis in patients with squamous cell

carcinoma of the tongue. Oral Oncol 47(7): 609-614, 2011. DOI: 10.1016/j.oraloncology.2011.05.006

10 Lim JY, Yoon SO, Hong SW, Kim JW, Choi SH, Cho JY: Thioredoxin and thioredoxin-interacting protein as prognostic markers for gastric cancer recurrence. World J Gastroenterol 18(39): 5581-5588, 2012. DOI: 10.3748/wjg.v18.i39.5581

11 Noike T, Miwa S, Soeda J, Kobayashi A, Miyagawa S: Increased expression of thioredoxin-1, vascular endothelial growth factor, and redox factor-1 is associated with poor prognosis in patients with liver metastasis from colorectal cancer. Hum Pathol 39(2): 201-208, 2008. DOI: 10.1016/j.humpath.2007.04.024

12 Chen Y, Ning J, Cao W, Wang S, Du T, Jiang J, Feng X, Zhang B: Research progress of TXNIP as a tumor suppressor gene participating in the metabolic reprogramming and oxidative stress of cancer cells in various cancers. Front Oncol 10: 568574, 2020. DOI: 10.3389/fonc.2020.568574

13 Guo X, Huang M, Zhang H, Chen Q, Hu Y, Meng Y, Wu C, Tu C, Liu Y, Li A, Li Q, Zhou P, Liu S: A pan-cancer analysis of thioredoxin-interacting protein as an immunological and prognostic biomarker. Cancer Cell Int 22(1): 230, 2022. DOI: 10.1186/s12935-022-02639-2

14 Hoshikawa H, Kamitori K, Indo K, Mori T, Kamata M, Takahashi T, Tokuda M: Combined treatment with D-allose, docetaxel and radiation inhibits the tumor growth in an *in vivo* model of head and neck cancer. Oncol Lett 15(3): 3422-3428, 2018. DOI: 10.3892/ol.2018.7787

15 Saydjari R, Alexander RW, Barranco SC, Townsend CM Jr, Thompson JC: The effects of 2-Deoxy-D-Glucoseand α-Difluoromethylornithine on the growth of pancreatic cancer *in vivo*. Pancreas 4(1): 38-43, 1989. DOI: 10.1097/00006676-198902000-00006

16 Maschek G, Savaraj N, Priebe W, Braunschweiger P, Hamilton K, Tidmarsh GF, De Young LR, Lampidis TJ: 2-Deoxy-d-glucose increases the efficacy of adriamycin and paclitaxel in human osteosarcoma and non-small cell lung cancers *in vivo*. Cancer Res 64(1): 31-34, 2004. DOI: 10.1158/0008-5472.can-03-3294

17 Stein M, Lin H, Jeyamohan C, Dvorzhinski D, Gounder M, Bray K, Eddy S, Goodin S, White E, Dipaola RS: Targeting tumor metabolism with 2-deoxyglucose in patients with castrate-resistant prostate cancer and advanced malignancies. Prostate 70(13): 1388-1394, 2010. DOI: 10.1002/pros.21172

18 Raez LE, Papadopoulos K, Ricart AD, Chiorean EG, Dipaola RS, Stein MN, Rocha Lima CM, Schlesselman JJ, Tolba K, Langmuir VK, Kroll S, Jung DT, Kurtoglu M, Rosenblatt J, Lampidis TJ: A phase I dose-escalation trial of 2-deoxy-d-glucose alone or combined with docetaxel in patients with advanced solid tumors. Cancer Chemother Pharmacol 71(2): 523-530, 2013. DOI: 10.1007/s00280-012-2045-1

19 Mitani T, Hoshikawa H, Mori T, Hosokawa T, Tsukamoto I, Yamaguchi F, Kamitori K, Tokuda M, Mori N: Growth inhibition of head and neck carcinomas by D-allose. Head Neck 31(8): 1049-1055, 2009. DOI: 10.1002/hed.21070

20 Indo K, Hoshikawa H, Kamitori K, Yamaguchi F, Mori T, Tokuda M, Mori N: Effects of d-allose in combination with docetaxel in human head and neck cancer cells. Int J Oncol 45(5): 2044-2050, 2014. DOI: 10.3892/ijo.2014.2590

21 Tohi Y, Taoka R, Zhang X, Matsuoka Y, Yoshihara A, Ibuki E, Haba R, Akimitsu K, Izumori K, Kakehi Y, Sugimoto M: Antitumor effects of orally administered rare sugar D-Allose in bladder cancer. Int J Mol Sci 23(12): 6771, 2022. DOI: 10.3390/ijms23126771

22 Noguchi C, Kamitori K, Hossain A, Hoshikawa H, Katagi A, Dong Y, Sui L, Tokuda M, Yamaguchi F: D-Allose inhibits cancer cell growth by reducing GLUT1 expression. Tohoku J Exp Med 238(2): 131-141, 2016. DOI: 10.1620/tjem.238.131

23 Wu Y, Sarkissyan M, Mcghee E, Lee S, Vadgama JV: Combined inhibition of glycolysis and AMPK induces synergistic breast cancer cell killing. Breast Cancer Res Treat 151(3): 529-539, 2015. DOI: 10.1007/s10549-015-3386-3

24 Vincent EE, Coelho PP, Blagih J, Griss T, Viollet B, Jones RG: Differential effects of AMPK agonists on cell growth and metabolism. Oncogene 34(28): 3627-3639, 2015. DOI: 10.1038/onc.2014.301

25 Chen W, Guéron M: The inhibition of bovine heart hexokinase by 2-deoxy-d-glucose-6-phosphate: characterization by 31P NMR and metabolic implications. Biochimie 74(9-10): 867-873, 1992. DOI: 10.1016/0300-9084(92)90070-u

26 Motoshima H, Goldstein BJ, Igata M, Araki E: AMPK and cell proliferation—AMPK as a therapeutic target for atherosclerosis and cancer. J Physiol 574(Pt 1): 63-71, 2006. DOI: 10.1113/jphysiol.2006.108324

27 Li J, Yue Z, Xiong W, Sun P, You K, Wang J: TXNIP overexpression suppresses proliferation and induces apoptosis in SMMC7221 cells through ROS generation and MAPK pathway activation. Oncol Rep 37(6): 3369-3376, 2017. DOI: 10.3892/or.2017.5577

28 Malm SW, Hanke NT, Gill A, Carbajal L, Baker AF: The anti-tumor efficacy of 2-deoxyglucose and D-allose are enhanced with p38 inhibition in pancreatic and ovarian cell lines. J Exp Clin Cancer Res 34(1): 31, 2015. DOI: 10.1186/s13046-015-0147-4

29 Kennedy CR, Tilkens SB, Guan H, Garner JA, Or PM, Chan AM: Differential sensitivities of glioblastoma cell lines towards metabolic and signaling pathway inhibitions. Cancer Lett 336(2): 299-306, 2013. DOI: 10.1016/j.canlet.2013.03.020

30 Jain VK, Kalia VK, Sharma R, Maharajan V, Menon M: Effects of 2-deoxy-D-glucose on glycolysis, proliferation kinetics and radiation response of human cancer cells. Int J Radiat Oncol Biol Phys 11(5): 943-950, 1985. DOI: 10.1016/0360-3016(85)90117-8

31 Tan MH, Alquraini H, Mizokami-Stout K, MacEachern M: Metformin: from research to clinical practice. Endocrinol Metab Clin North Am 45(4): 819-843, 2016. DOI: 10.1016/j.ecl.2016.06.008

32 Cheong JH, Park ES, Liang J, Dennison JB, Tsavachidou D, Nguyen-Charles C, Wa Cheng K, Hall H, Zhang D, Lu Y, Ravoori M, Kundra V, Ajani J, Lee JS, Ki Hong W, Mills GB: Dual inhibition of tumor energy pathway by 2-deoxyglucose and metformin is effective against a broad spectrum of preclinical cancer models. Mol Cancer Ther 10(12): 2350-2362, 2011. DOI: 10.1158/1535-7163.MCT-11-0497

33 Goodwin PJ, Chen BE, Gelmon KA, Whelan TJ, Ennis M, Lemieux J, Ligibel JA, Hershman DL, Mayer IA, Hobday TJ, Bliss JM, Rastogi P, Rabaglio-Poretti M, Mukherjee SD, Mackey JR, Abramson VG, Oja C, Wesolowski R, Thompson AM, Rea DW, Stos PM, Shepherd LE, Stambolic V, Parulekar WR: Effect of metformin vs placebo on invasive disease-free survival in patients with breast cancer: the MA.32 randomized clinical trial. JAMA 327(20): 1963-1973, 2022. DOI: 10.1001/jama.2022.6147

34 Kennedy OJ, Kicinski M, Valpione S, Gandini S, Suciu S, Blank CU, Long GV, Atkinson VG, Dalle S, Haydon AM, Meshcheryakov A, Khattak A, Carlino MS, Sandhu S, Larkin J, Puig S, Ascierto PA, Rutkowski P, Schadendorf D, Boers-Sonderen M, Di Giacomo AM, van den Eertwegh AJM, Grob JJ, Gutzmer R, Jamal R, van Akkooi ACJ, Robert C, Eggermont AMM, Lorigan P, Mandala M: Prognostic and predictive value of metformin in the European Organisation for Research and Treatment of Cancer 1325/KEYNOTE-054 phase III trial of pembrolizumab versus placebo in resected high-risk stage III melanoma. Eur J Cancer 189: 112900, 2023. DOI: 10.1016/j.ejca.2023.04.016

35 Raez LE, Papadopoulos K, Ricart AD, Chiorean EG, Dipaola RS, Stein MN, Rocha Lima CM, Schlesselman JJ, Tolba K, Langmuir VK, Kroll S, Jung DT, Kurtoglu M, Rosenblatt J, Lampidis TJ: A phase I dose-escalation trial of 2-deoxy-d-glucose alone or combined with docetaxel in patients with advanced solid tumors. Cancer Chemother Pharmacol 71(2): 523-530, 2013. DOI: 10.1007/s00280-012-2045-1

36 Mohanti BK, Rath GK, Anantha N, Kannan V, Das BS, Chandramouli BA, Banerjee AK, Das S, Jena A, Ravichandran R, Sahi UP, Kumar R, Kapoor N, Kalia VK, Dwarakanath BS, Jain V: Improving cancer radiotherapy with 2-deoxy-d-glucose: phase I/II clinical trials on human cerebral gliomas. Int J Radiat Oncol 35(1): 103-111, 1996. DOI: 10.1016/s0360-3016(96)85017-6

37 Singh D, Banerji AK, Dwarakanath BS, Tripathi RP, Gupta JP, Mathew TL, Ravindranath T, Jain V: Optimizing cancer radiotherapy with 2-Deoxy-D-glucose. Strahlenther Onkol 181(8): 507-514, 2005. DOI: 10.1007/s00066-005-1320-z

Received February 28, 2024
Revised March 21, 2024
Accepted March 22, 2024